

A Testbed for Studying High Voltage Battery Management Systems (BMS) and their Integration into Shipboard Control Systems*

Cole Tschritter¹, David A. Wetz¹, PhD, Alexander N. Johnston¹, and John M. Heinzl², PhD

¹*Univ. of Texas at Arlington (UTA), Electrical Engineering Department, 416 Yates Street, Rm. 537, Arlington, TX 76019 USA*

²*Naval Surface Warfare Center – Philadelphia Division, 5001 S Broad St, Philadelphia, PA 19112 USA*

Synopsis

Lithium-ion energy storage is being considered as either a prime power source, backup power source, or buffering source in next-generation shipboard and automotive power systems. Open circuit potentials as high as 1 kVDC are proposed and while high voltage batteries are emerging in industrial solar applications and even in automobiles, their deployment is limited. There is much to learn about how to assemble batteries with this high a voltage and how to ensure they are safely operated, maintained, and integrated with existing shipboard power system controllers. Battery management systems (BMS) serve as the primary hardware and software level control to monitor, manage, and operate lithium-ion batteries. There are countless BMSs available commercially and tools are needed to study each one in safe and efficient manner. In the work presented here, a battery emulator has been assembled and validated using a power-hardware-in-the-loop (PHIL) system. Using this method, any type of battery can be emulated so long as a validated MATLAB simulation model at the cell level is available. Hardware is being procured to expand the system so that a 264-cell battery can be emulated. The options considered for emulation of the real-time battery model will be discussed along with some experimental results obtained to date.

Keywords: Energy Storage, Power System Controls, Energy Management

1. Introduction: 1000V Batteries and Battery Management Systems

Batteries are an integral part of modern-day electronics and are fielded in a wide variety of devices and systems. Despite the varying design, chemistry, and ratings, batteries have boasted a high safety track record overall. They are fielded as primary power sources as well as buffers within countless applications, including shipboard power systems. High potential batteries are assembled using multiple cells connected in an n series and m parallel configuration. Batteries with voltages as high as 1 kVDC, which requires approximately ~265 battery cells to be connected in series, are being considered for use as sources in future zonal shipboard power system architectures (Wetz 2016, Dodson 2019) and vehicles (Moloughney 2021), among other applications. Battery voltages as high as 1 kVDC have been previously demonstrated (Wetz 2016, Dodson 2019, Moloughney 2021) but they are limited. Buffering transient loads or high priority loads with a battery in the absence of an alternative power source is critical to the future deployment of more electrical loads aboard next generation ships.

A Battery Management System (BMS) is responsible for monitoring and maintaining the individual cells of a battery. The primary task of a BMS is to monitor the voltage, or State of Charge (SoC), of each respective cell and if something falls outside of a safe range of operation, it should either autonomously change the mode of operation such that safety can be restored, or it should report the unsafe operation to an overarching controller that will do so (Buccolini 2018, Colthorpe 2022). When cells are at a higher SoC then they should be to maintain balance among all the cells, the BMS should operate balance circuits that dissipate energy from those cells. As already described, modules of a battery are typically assembled by wiring cells in a n series and m parallel (nS/mP) configuration, increasing the voltage and current capabilities of the battery respectively. Each module will typically have its own

monitoring and balance circuit card. A higher-level card is typically used to facilitate communication amongst the different module level cards and to control the operation of the battery. Figure 1 illustrates an example of this architecture. Even if the batteries connection to a bus is autonomously handled by the BMS, it should still be integrated with the shipboard power system's controller to ensure reliability and safety. In the work documented here, a battery emulator has been configured to be used as a way of studying high-voltage battery operation, BMS operation across all possible scenarios, and integration of the BMS into a host power system controller.

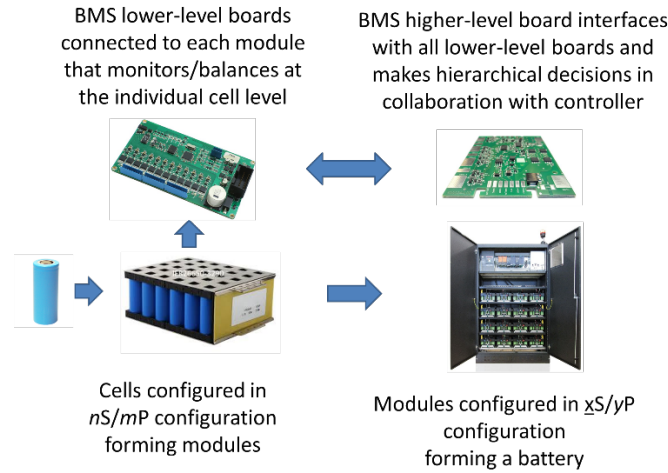


Figure 1. Example battery and BMS architecture.

BMSs typically come in two different types, active and passive. An active BMS topology can recharge lower SoC cells using the energy removed from higher SoC cells and have been documented and studied (Cao 2008). Passive topologies are where cells' excess energy is dissipated as heat. This prevents overcharging cells and balances the cells down. Figure 2 contains three examples of passive topologies, above, which utilize a resistor to dissipate the energy, as well as two active topologies, below, that shuttle charge between cells. Focusing on passive topologies, they frequently balance down to a user pre-defined set point or to the lowest measured cell voltage. Typical balance circuits dissipate current in the few mA to a few hundred mA range. When the charge current significantly exceeds the balance current, the BMS is unable to bleed current quickly enough from the high cells and the charger must be cut off from the battery before all cells have been sufficiently charged to prevent the highest cell from entering thermal runaway. BMSs with higher balance currents, in the few A range, have been designed to speed up the balance process but they can get bulky, add significant cost, and can require cooling of their own if the thermal design is not adequate.

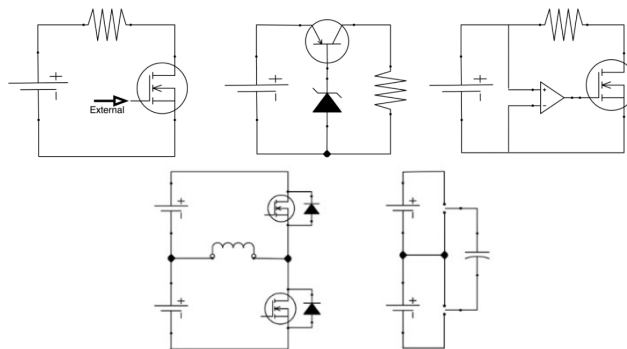


Figure 2. Example of passive balancing topologies. Bleed resistor with externally driven MOSFET (upper left), passive transistor biased with zener diode (upper middle), bleed resistor with locally driven MOSFET using comparator (upper right). Example of active balancing topologies. Inductor based boost mode active balancing (lower left) and capacitor-based charge shuttle active balancing (lower right).

In addition to balancing cells, BMSs perform many critical functions. More expensive BMSs are usually able to monitor individual cell voltages and report them to a host controller. Each lower-level board is typically able to measure no more than a few temperature measurements from thermocouples or thermistors attached to selected point(s) of interest within the module to indicate if higher than acceptable temperatures are present. If any cell is over-discharged, over-charged, or if any temperature threshold is exceeded, the BMS can interface with an output relay, enabling the battery to be isolated from the source or load till safe conditions can be restored. If the BMS is not interfaced directly with an output relay, the shipboard control system can utilize the information from the BMS to manage the battery's operation in the power system.

Each BMS manufacturer boasts of an improved balance topology, control algorithm, communication strategy, cooling technology, interface method, etc. to encourage customers to use their BMS. Since there are no standards by which all BMSs are designed and tested against, it is critical for the intended user to be able to evaluate the short- and long- term performance of a BMS before it is installed on a battery. Should a BMS not work as advertised, the result could be very costly at best and very dangerous at worst (Cummings 2022, IRCLASS 2022, BMS Failure 2022, Chung 2022). Shipboard controls need to be developed to interface with a BMS and properly control the battery in all use cases of the power system. In the work performed here, a high voltage battery is emulated using power-hardware-in-the-loop (PHIL). The emulated battery can be interfaced with any typical BMS so that it can be evaluated and studied. Though only a few cells have been demonstrated using PHIL to date, the intended goal of the testbed is to be able to emulate batteries with as many as 264 individual cells and potentials as high as ~1 kVDC. The ability to dynamically adjust each individual cell's SoC in real-time allows both normal and abnormal conditions to be tested safely and rapidly. This capability reduces the knowledge gap that exists in understanding the potential problems that come with high voltage battery and BMS operation within next generation shipboard power systems.

2. Testbed Designs

Many different options were considered for emulating a 264-cell battery. These options have been discussed in more depth previously (Tschrirter 2021). The most pertinent options will be discussed briefly below.

2.1. Commercial Battery Emulators

Several battery cell emulators are available commercially from vendors such as Chroma Systems (Chroma 2019), Hioki USA (Hioki 2020), and Speedgoat Inc. (Speedgoat 2021), respectively. The increased demand for batteries in electric vehicles and grid energy storage has led to the demand for these types of cell emulators and they have good capability and functionality for this type of application. The Chroma 87001 and Speedgoat IO991 units have been studied in the work documented here.

2.1.1. Chroma 87001

The Chroma 87001 battery emulator has sixteen channels per unit, each of which has a usable voltage range from 0 VDC – 5 VDC and a source/sink current as high as 5 A continuously. The datasheet lists a galvanic isolation as high as 2000 VDC meaning that thirty – 16 cell units can be assembled in series to emulate batteries with as many as 480 cells. Figure 3 presents a visual one-line diagram of this hardware would be used in the battery emulator studied here. Chroma offers a proprietary battery software emulation that is used to configure each channel with a response time of 1 ms. The software allows the user to input parameters represent the cell of interest but it would not be a validated representation in the same way an HIL model would be. A standard Ethernet connection can be used to remotely control each channel with a response time around 10 ms. Each additional unit daisy chained to the target computer will add an estimated 10 ms to the response time. Tests on a single Chroma unit has shown this to be a viable option and single unit evaluation has been performed using a Chroma 87001 emulator. Some results will be shown later. This is a viable option that has been considered for the full 1 kVDC testbed but it is not the one chosen for procurement here.

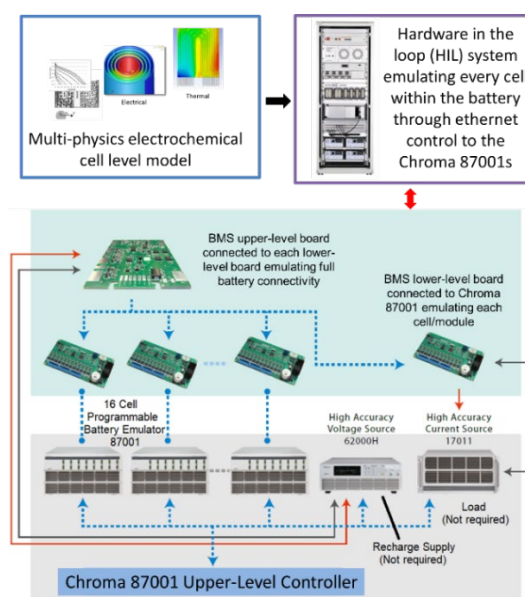


Figure 3. Visual one-line diagram of a testbed layout employing multiple Chroma 87001 cell emulators.

2.1.2. Speedgoat IO991

Speedgoat offers an integrated battery emulator solution that is slightly different than the respective units offered by either Chroma or Hioki. Speedgoat's IO991 module has six channels that can output 0 – 7 VDC, sink 100 mA, and source 300 mA. Their current model is limited to 750 VDC of galvanic isolation, falling well short of the 1000 VDC target voltage. The IO991 modules are assembled into a one or more multi-slot PXI chassis and then stacked in series. Speedgoat's advantage comes in its immediate ability to emulate an HIL battery model developed in MATLAB/Simulink. Speedgoat's cell emulation hardware is designed to interface with its HIL target platform that instructs each channel of the IO991. Speedgoat hardware is designed to interface seamlessly with its own target HIL machine using their own software block sets; however, it is possible to interface the IO991 card on another system with a PXI connection. This is unlike the Chroma and Hioki systems that interface through a standard Ethernet interface. Figure 4 describes the employment of the IO991 units in the BMS testbed being developed here. Three IO991 cards have been obtained from Speedgoat and demonstrated. A few results will be shown later.

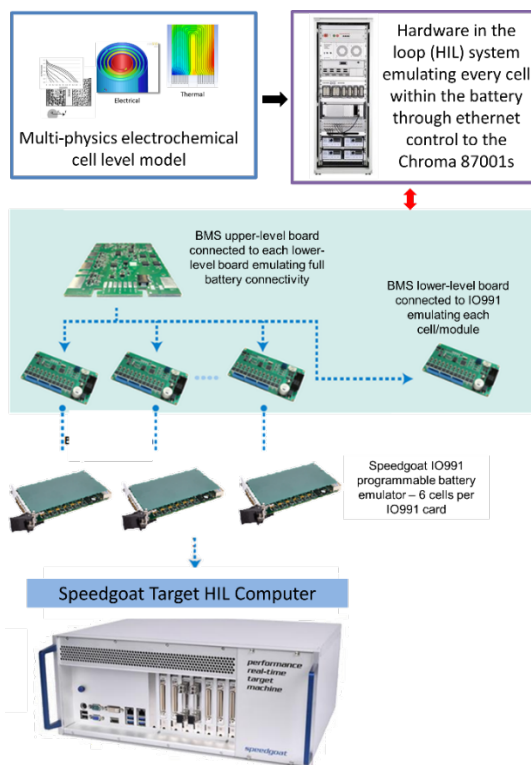


Figure 4. Visual one-line diagram of a testbed layout employing multiple Speedgoat IO991 cell emulators.

2.1.3. Speedgoat BCE proto-type

Speedgoat is currently developing a new revision of their battery emulator that will have a galvanic isolation higher than 1 kVDC, the final number still being determined, channel voltage of 0 – 5 VDC, and channel source/sink current of 5 A per channel. It will communicate through a standard Ethernet connection like the Hioki and Chroma emulators; however, it will differ in that a block set is being developed that can readily be used to handle communications and settings, rather than manual TCP commands that would have to be done in the HIL model. It is estimated to have a 10 ms response rate for the commands and built-in current sense. This design is anticipated to be available in late 2022 and is the one ultimately chosen for emulation of a 264-cell battery. Because it is still in the prototype phase, no results from it will be shown here.

2.1.4. Hardware Option Comparison

A comparison the capabilities of each of the four commercial solutions is presented in Table 1. Chroma, Hioki, and Speedgoat have all demonstrated the use of their emulators for studying BMSs, in a manner like the way they are being studied here. A primary focus of the work performed here is the use of a validated HIL multi-physics battery model, allowing the user to study their cell at a very detailed level, rather than relying on a generic model. Understanding the hardware and processing requirements for emulating a multi-physics model is a primary goal. All three of these commercial systems seem viable for the intended application at the 1000 VDC level, except for the Speedgoat IO991 which is voltage limited. Preliminary work has been performed using three of Speedgoat's IO991 modules, and a single Chroma emulator.

Table 1. Summary of the hardware capabilities offered by Chroma Systems, Hioki, and Speedgoat, respectively.

Battery Emulator	Chroma 87001	Hioki SS7081-50	Speedgoat IO991	Speedgoat BCE Prototype
Channels per Lower-Level Device	16	12	6	12
Cell/Channel Voltage	0 V - 5 V	0 V - 5.1 V	0 V - 7 V	0-5V
Cell/Channel Sink Current	5 A	1 A	100 mA	5A
Cell/Channel Source Current	5 A	1 A	300 mA	5A
Cell/Channel Voltage Accuracy	(0.02%FS) ±1 mV	±0.0150% ±500 μV	±0.2% ±20 mV	±0.01% ±0.5 mV
Voltage Isolation	1000 V ch-ch, 2000 V to gnd	1000 V	750 V	96 V ch-ch 1600 V to gnd

3. Experimental Setup and Results

3.1. Model Deployment in HIL

As described already, it is intended that multi-physics battery models will be able to be developed in MATLAB/Simulink and emulated using the PHIL platform. A few of these models have been developed and are being used in the testbed with excellent results so far. The ones being used contain some proprietary properties that are not publishable at this time and therefore they cannot be presented in detail here. A more generic battery model developed using the same technique in a Simulink environment is being used here to demonstrate functionality. There are two general ways to develop a battery model in Simulink. At the simplest level, the pre-installed Simulink models can be used that have customizable, chemistry dependent, settings entered easily by the user. Some of the models have options for calculating cell temperature and even state of health (SoH). The second way is for the user to develop their own mathematical or empirically derived model of their cell. This method gives the user complete control over the battery model and the level of detail captured by it. This latter method is the one of interest here and is the primary reason why PHIL capability is so critical to the testbed’s success. The former is being used here for simplicity of showing how the PHIL model is deployed to the emulator and how the BMS responds to rapid changes in SoC deployed by the emulator.

Though the Speedgoat hardware has been selected to initially emulate a battery, the Chroma and Hioki options are also appealing. The Chroma and Hioki hardware can be interfaced with any HIL target machine running MATLAB/ Simulink so the battery models being developed are deployable using Speedgoat and OPAL-RT HIL systems, respectively. The Speedgoat target machine connects to its hardware directly through Simulink Real-Time (RT). The OPAL-RT system uses RT - Lab to deploy models from Simulink. Deployment into the OPAL-RT system has been previously discussed (Tschritter 2021) so the data presented here will only expand on Simulink RT deployment. To deploy a model from Simulink to Speedgoat, a MATLAB add on for Simulink RT must be downloaded. When running this app, Simulink generates C code for RT operation. Once the model is ready for RT operation, Speedgoat’s IO991 modules can be configured to work with individual cell models. It’s possible to configure the settings in the IO991 modules before the model begins to run; however, this pre-model run configuration is not easily achievable on the Chroma system. The Chroma system is easier to initialize and configure with a user defined initialization sequence that begins after the Simulink model starts running. After it starts running, the user initialization function switches to operating the cell model. Part of the model responsible for commanding the Chroma unit is shown in Figure 5.

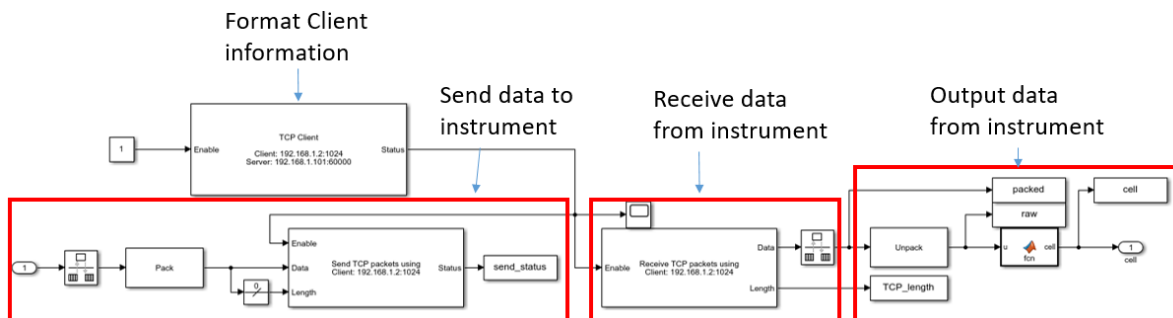


Figure 5. Ethernet interface designed to provide communication between the HIL battery model and the cell emulator hardware. It is currently used with the Chroma 87001 emulator; however, this subsystem should be compatible with other instruments and emulators that communicate using this method.

The model has been deployed on the Speedgoat HIL and Speedgoat IO991 modules utilizing multiple instances of a generic Simulink cell model connected in series. The cell models are assembled as 10S modules and then 26 of those modules are connected in series to make up the simulated battery. A 27th module with only 4 series cells is included to bring the total number up from 260 cells to the full 264 cells, which is the number of channels that have been procured but not yet received. An example constant current discharge of the 264 cells is shown in Figure 6. Each individual cell's voltage will eventually be emulated using its own emulator channel. As will be shown, the emulators will be interfaced with different low-level BMS cards, whose performance is able to be evaluated in RT.

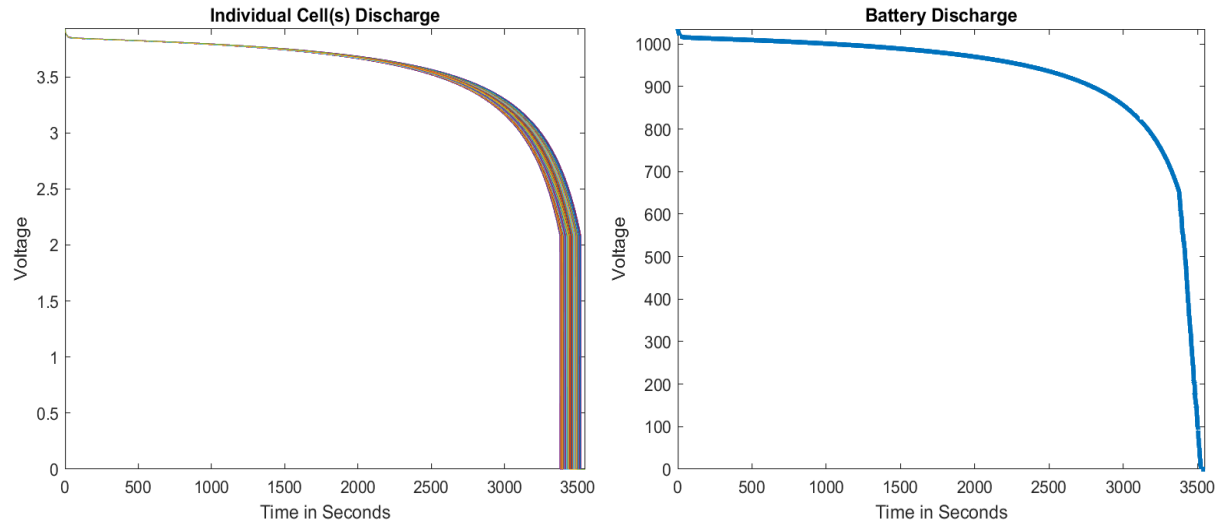


Figure 6. Battery discharge curves. Left graph shows identical cells starting at slightly different SoCs ($93\pm 2\%$) discharging at the same C rate. The slight change in SoC can cause dramatic changes in the voltage over time. The right graph shows the sum of these voltages, representing the full battery voltage.

In a real battery, it is impossible for a cell's SoC to suddenly change by a rapid amount safely. When using cell emulators, it is possible to rapidly change a cell's SoC to evaluate how a BMS responds at each voltage limit and above or below a balance limit quickly, without waiting for a proper charge or discharge procedure to occur. This is achieved by introducing functionality that allows the user to independently adjust each individual cell's SoC in RT. To do this, a custom MATLAB application was developed that lets the user adjust the SoC of the individual cells during runtime without having to recompile the model and without diminishing the model's performance. The application is shown in Figure 7 as a matrix with each individual cell's SoC that is adjustable by the user.

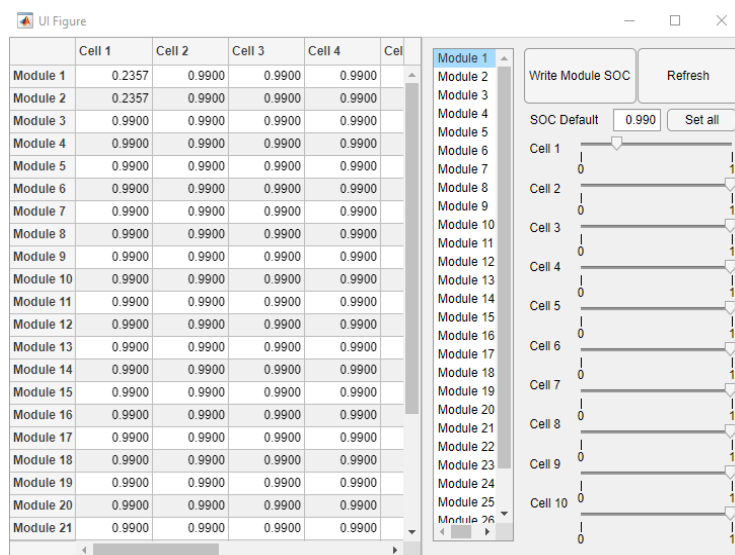


Figure 7. Custom MATLAB application used to change the SoC of each individual cell in real time.

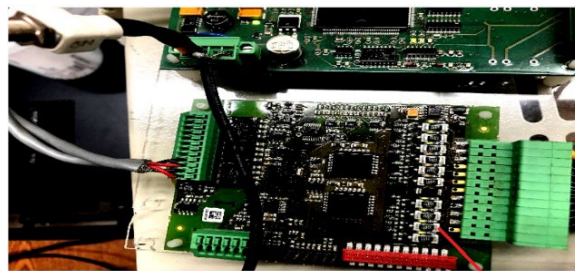
3.2. Connection of the Speedgoat IO991 to a Low-Level BMS Board

To date, a few different BMSs have been briefly studied using three 6-cell Speedgoat IO991 emulator modules and a single Chroma 87001 16-cell emulator. Three IO991 modules, seen in Figure 8, are available and this restricts deployment to no more than 18 cells at the time. A photograph showing a lower-level 10-cell BMS board connected to the IO991 modules is shown in Figure 9. Using the application described earlier, each individual cell's SoC can

be changed in RT by the user or through execution of normal charge or discharge routines within the simulation. Though the model is running in RT with 264 cells being simulated, only 10 are being deployed to the emulator. The BMS studied in Figure 9 is one that was on hand from a previous experiment. This BMS is a passive design that balances down to the module's lowest cell voltage, so it is always balancing if the cells SoCs are not close to each other. Though not shown here, a higher level BMS board is interfaced with a PC running a National Instruments LabView Virtual Instrument (VI) to monitor each individual cell's voltage in RT. When a battery is deployed in the field, this type of VI can be used to interface with other control systems that ensure the battery is never connected to a source or load if a cell falls outside of its acceptable range of operation.



Figure 8. Speedgoat expansion chassis with three IO991 emulator cards.



Balance Resistors and LEDs

Figure 9. Lower-level BMS board balancing cells emulated by the IO991 cards. LEDs indicate cells 1-3 and 7-10 are balancing while cells 4-6 do not need balancing.

When a cell needs to bleed down, a $80\ \Omega$ resistor is connected in series with it along with an LED that lights up, seen in Figure 9. The IO991 can source up to 100 mA, well within the balance current that even a fully charged cell emulator can supply when balancing. A problem with the IO991 card is that it does not have any internal current monitoring so without an external current measurement there is no feedback into the RT model that updates the SoC based off current supplied or added to a cell. Feedback has been introduced using a custom designed circuit board that is connected in series between the IO991 and the BMS, seen in Figure 10. The board places a $0.1\pm 1\%\ \Omega$ current sense resistor in series with each cell and across each current sense resistor there is a differential voltage monitor whose output is fed into a Speedgoat IO323 analog input card. That measurement is used in RT to back out the current sourced in or out of the cell whose SoC is updated. The latest revision of the current sense board is shown in Figure 10 and, as will be shown next, it is working well.

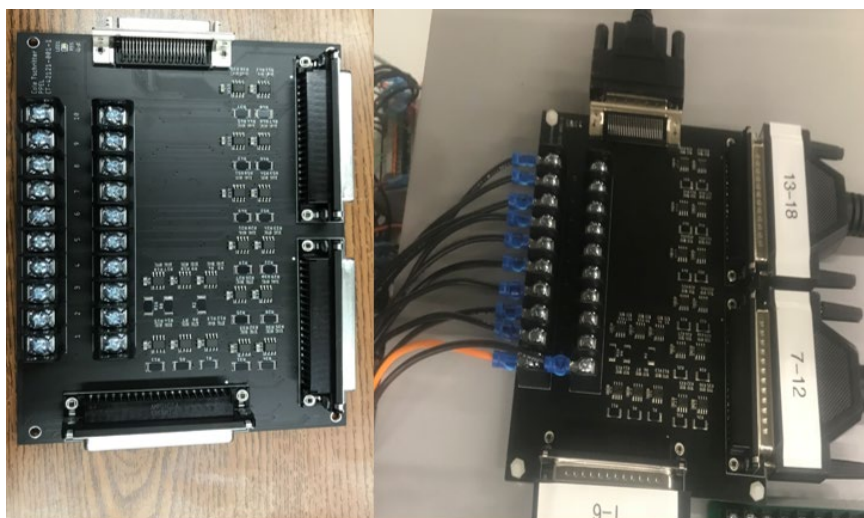


Figure 10. Populated current sense board and attached between the cell emulator and the lower level BMS card. Up to 18 cells can be outputted and sensed with this design. A variable gain selected by adjusting a resistor network. Modular design allows for quick connect and disconnect from the IO991 cell emulators and IO323 measurement cards.

3.3. Data Collected from Emulated Cells

3.3.1. Preliminary data prediction

Data demonstrating the balancing of emulated cells and the ability to rapidly alter cell SoC will be shown here. As a precursor to showing hardware operation, two computer drawn graphs illustrating predicted operation in a few different scenarios are shown in Figure 11. The discussion will focus on the upper graph first. In the first green section, a normal charge routine is shown where two series connected cells are clearly unbalanced. The higher SoC cell reaches its maximum charge voltage of 3.65 V, causing the charge cycle to stop, after which the balance process is clearly visible. Note that in this graphic, it is assumed that the recharge current is much greater than the balance current so there is no noticeable change in the charge current after it exceeds the balance voltage threshold, but the balance circuit would engage at that point to bleed off excess energy. Depending on the capability of the BMS, cell voltage information will be visible in RT by the shipboard power system controller as well. Having this information during a recharge will allow it to predict that the BMS will soon be cutting off the battery, dropping load from the power system. If it's normal operation, the controller will reconfigure the power system to anticipate the dropped load and if it's not normal operation, it can decide the best course of option to prevent further problems. When the balance voltage is reached, the charge process is restarted, something that again should be anticipated by the power system controller to accommodate the load that is about to come on. In the first pink section, a discharge process is shown where two series cells are discharging at different rates due to them having different internal resistances. When a cell reaches its minimum allowable voltage, the discharge process is halted, something the power system controller again needs to be able to anticipate and possibly prepare for. A similar recharge process as that described already is repeated in the next green section and a combined discharge and recharge cycle is shown in the next blue section.

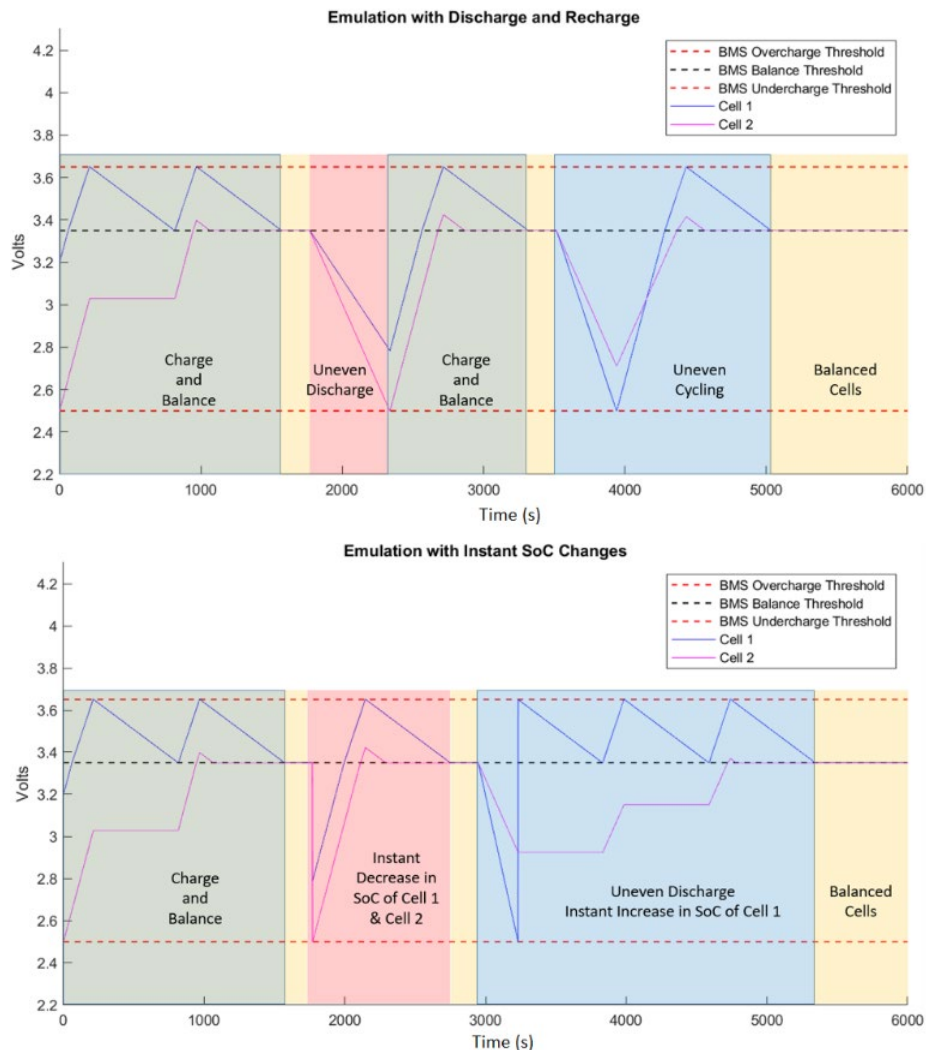


Figure 11. Predicted BMS behaviour with two cells. Top graph shows simplified charge/discharge and balance profiles during normal operation. The lower graph demonstrates the user's ability to rapidly change individual cell(s) SoC to evaluate BMS behaviour quickly.

In the lower graph, the same charge and balance process is shown in the first green section. In the pink section, the ability to rapidly change one or more cell's SoC is shown, something not possible with physical batteries under normal or safe operation. If something like this were to occur, it would more than likely be something bad happening that the shipboard power system controller must be ready to respond to. Both cell's SoC is rapidly decreased demonstrating how the BMS should measure the minimum allowable voltage and disconnect the battery from a source or load. In the next blue section, a rapid increase in one cell's SoC up to the maximum allowable voltage is shown. When this occurs, the battery is again isolated from a source or load and the balance process begins on the high SoC cell. After this, a few normal charge and balance processes are shown. Using the emulator to study this type of operation allows the BMS to be studied and the shipboard controller's response to both normal and abnormal battery operation.

3.3.2. Speedgoat IO991 Emulators on Actia BMS

Having demonstrated what is expected, a few preliminary results from the emulator hardware setup so far will be shown. Figure 12 shows the measured voltages and balance currents measured from 5 of the 10 cells emulated using the IO991 that are interfaced with the BMS seen in Figure 9, made by Actia. Data from only five cells is shown to make the graphs a little easier to read, however the BMS is managing all ten of the emulated cells. The model is at rest and is not connected to any source or load so only cell balancing is occurring. Cells 1, 2, and 3 are each set to the same SoC of 55%. Cell 5 is set significantly higher than the rest, near 100%, and Cell 4 is set somewhere in between them all at roughly 85%. Because cells 4 and 5, respectively, are so much higher than the other three, their balance circuits are continuously held on and roughly 45 mA is drawn by the BMS to balance them down. As current is drawn by the BMS, it is measured by the sense circuit and fed back into the model so that output voltage is adjusted according to the new SoC. Cells 3, 4, and 5 exhibit interesting behaviour. Because this BMS is designed to balance down to the lowest cell within the module and not a set threshold, there is a hysteresis effect that is visible. As the voltage sense circuit in the BMS fluctuates slightly, the similar voltages cause the processor to alternate whose voltage is higher. This causes the balance to turn on and off in a switched manner. The plot simply demonstrates the ability to emulate cells and evaluate the balance current of the BMS. Though not shown here, the cell voltages are reported by the BMS to a host controller being run in NI LabVIEW. This controller represents a shipboard power system controller that would be monitoring the battery SoC and using that to ensure safe operation.

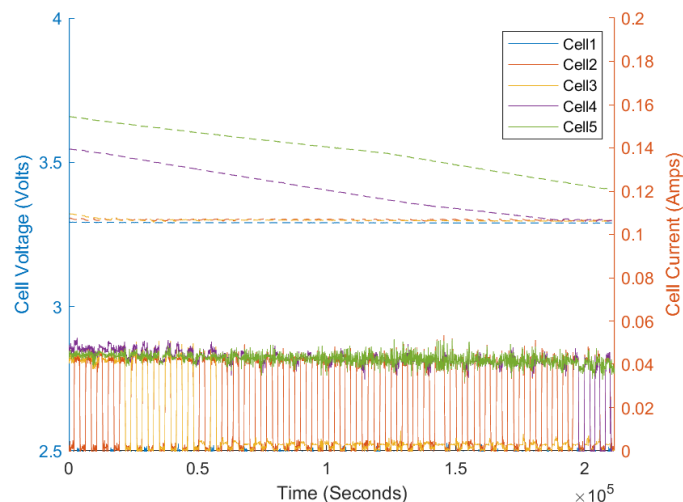


Figure 12. Voltage and current data collected while five emulated cells are connected and balanced by the BMS. Solid lines indicate cell current while dashed lines represent cell voltages. The data demonstrates the BMS balance circuits engaging and balancing down the cell(s) whose potentials are higher than the module's cell that has the lowest voltage.

In Figure 13, the ability to rapidly change a cell's SoC is demonstrated. At the beginning of data collection, each cell's SoC is set to 55%. The SoCs of Cell 2, Cell 4 and Cell 5 were manually increased to 60%, 85%, and 57% respectively at random times between 50,000 s and 100,000 s into the simulation. Each time the SoC of a cell is raised above the minimum cell voltage, the cell's balance circuit engages drawing current. Because Cell 1 and Cell 3 remain at the same SoC, they exhibit the same hysteresis behavior seen earlier and once cells that are higher balance down, they do so as well. The ability to rapidly change a cell's SoC like this is something that cannot happen in real life, significantly decreasing the time needed to fully evaluate how a BMS behaves when cells are near their operational limits. It also enables the overvoltage performance of the BMS to be observed in a controlled way since it is not feasible to overcharge a live battery. Though this type of condition is not presented here, it is one that will be studied soon and especially once the full 264-cell battery is emulated. This capability will enable power system control software to be developed to properly accommodate these bounds of the battery's safe operation.

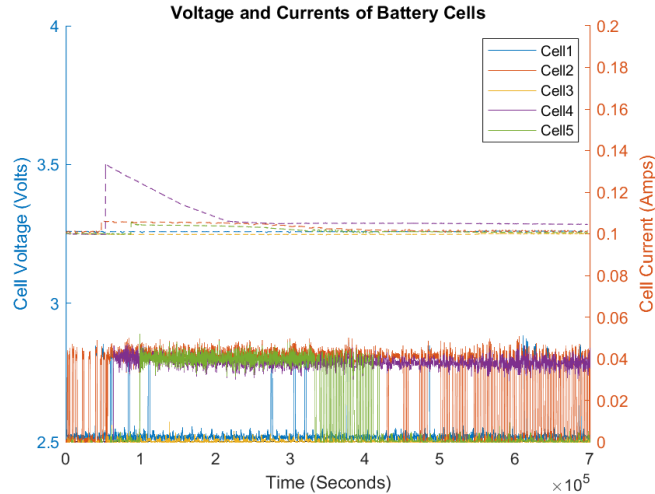


Figure 13. Voltage and current data collected while ten emulated cells are connected and balanced by the BMS. Only five cells are shown to increase visibility. Solid lines indicate cell current while dashed lines represent cell voltages. The data demonstrates the ability to rapidly change a cell(s) SoC to evaluate a BMS’s performance near cell bounds quickly.

3.3.3. *Speedgoat IO991 Emulators on K2 Energy BMS*

Next, the IO991 modules were tested on a BMS made by K2 Energy. This BMS is comprised of three PCBs used for balancing, monitoring, and communication, respectively. The first PCB is the high-level card, which handles all the secondary cards that attach to each module. It has a CAN communication output that is fed into a secondary communication board. The communication board attaches to the master and converts the CAN data to a fiber optic signal. This enables the BMS to be isolated from the larger power system controller and prevents electrical noise from interfering with communication link to the host controller. Lastly the BMS employs lower-level cards that each interface with its own 10S/mP module. Each BMS channel employs a 39 Ω balance resistor, so the balance current is just under 100 mA. The individual cell voltages are reported by the BMS to the LabVIEW host controller over the fiber link.

Data from the K2 Energy BMS collected over multiple cycles is seen in the leftmost plot of Figure 14. The BMS does not balance to the cell with the lowest recorded voltage, but rather it balances to a lower predefined voltage threshold. Before balancing occurs, cells must be charged. Once the initial balance threshold voltage is reached, balance circuits are engaged, and balancing begins. The recharge continues until any cell reaches the upper charge voltage limit and when this occurs, the BMS either disengages the charger or reports the end of charge command to the host controller so that it can stop the charge. The BMS balances the cells down to the balance threshold. In this experiment, balancing is allowed to occur until any cell reaches the lower balance threshold after which the battery is recharged again. In these experiments, the recharge is emulated in software. A zoomed-in plot showing one cycle is shown in the rightmost plot of Figure 14. The plots shown in Figure 14 demonstrate a significant amount of noise present on the output of the emulator channels. This is a concern that is being evaluated.

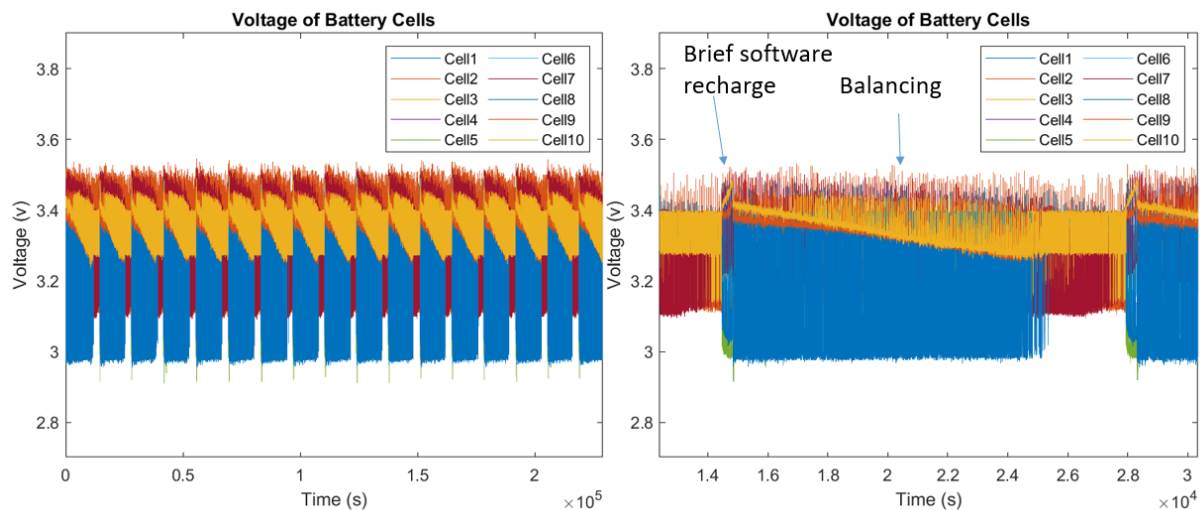


Figure 14. Experiment demonstrating balancing of the K2 Energy BMS. Multiple cycles are shown to bring the cells into proper balance. The left graph is a zoomed-out version showing multiple cycles while the right graph is a zoomed-in version of a single cycle. The test is performed using the IO991 emulator cards which have a significant amount of noise on them.

3.3.4. Chroma Emulator on K2 Energy BMS

The same K2 Energy BMS was also studied using the Chroma 87001 emulator. An example of the Chroma system being successfully brought into balance with a difference larger than 50% SoC between cells is seen in Figure 15. A reminder that the Chroma emulator is controlled using a network connection with a 10 ms response rate. Current sense is also built into the Chroma emulator and is fed back into the HIL to update each respective cell's SoC. Commands to the Chroma unit are sent one at a time. Setting the voltage of 16 cells takes 10 ms for each command and are stored in the emulator while an additional single command fetches the current sources/sink by each cell. A command to update the emulator output voltages causes the unit to output the stored values, resulting in a full update rate of 170 ms. A noticeable difference between the Chroma 87001 emulator and the Speedgoat IO991 emulator is the stability in the Chroma's output voltage. It is estimated the IO991 card has approximately ± 0.2 V of noise while the Chroma emulator has approximately ± 0.01 V of noise. This is a significant difference that needs to be further studied.

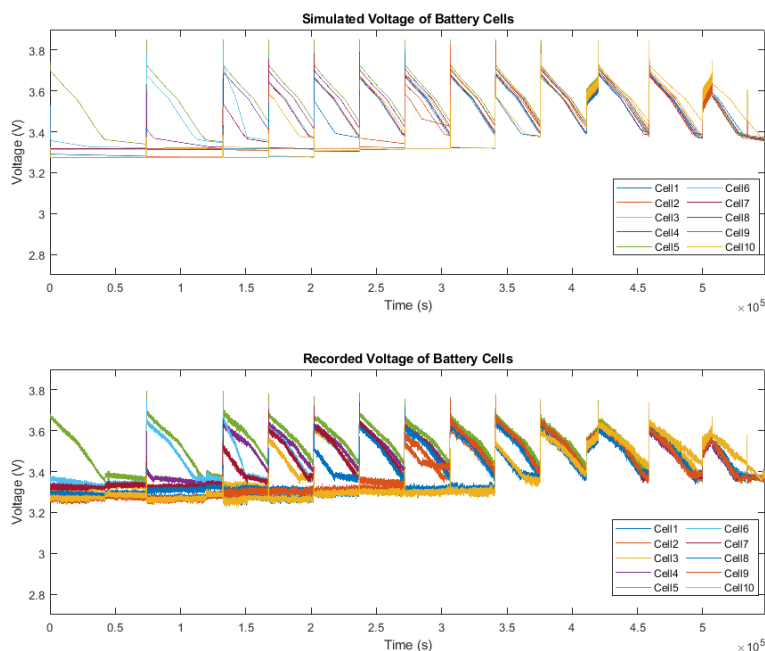


Figure 15. Chroma emulator being balanced by the K2 Energy BMS. The top graph contains the values commanded by Simulink while the bottom graph contains the voltage values reported by the BMS. The balance start threshold is set to 3.4 VDC while the balance end threshold is set to 3.35 VDC. The 3.8 VDC max recharge limit is set in Simulink. The battery appears to be balanced at approximately $3.75 \cdot 10^5$ seconds. At the start of the simulation, the highest cell was at a SoC of 98% SoC and the lowest cell was at 45% SoC.

Perhaps the most interesting result was obtained using the Chroma emulator when abnormal operation from the K2 Energy BMS was observed, seen in Figure 16. The BMS, seemingly from the start of the simulation, behaves oddly, discharging cells that are already below the lower balance threshold unexpectedly. The BMS continued to drain cells until they reached 0 VDC, not cutting off when the voltage is clearly below 3.35 VDC. This is exactly the behavior that could cause catastrophic damage to a battery. Being able to observe this and understand why it is happening is critical to properly controlling the battery. Detecting these anomalies in the shipboard power system controller and properly responding to them is something this work aims to demonstrate. Unfortunately, this error has not been observed a second time. The BMS will continue to be studied to identify what caused this behavior so it can be prevented.

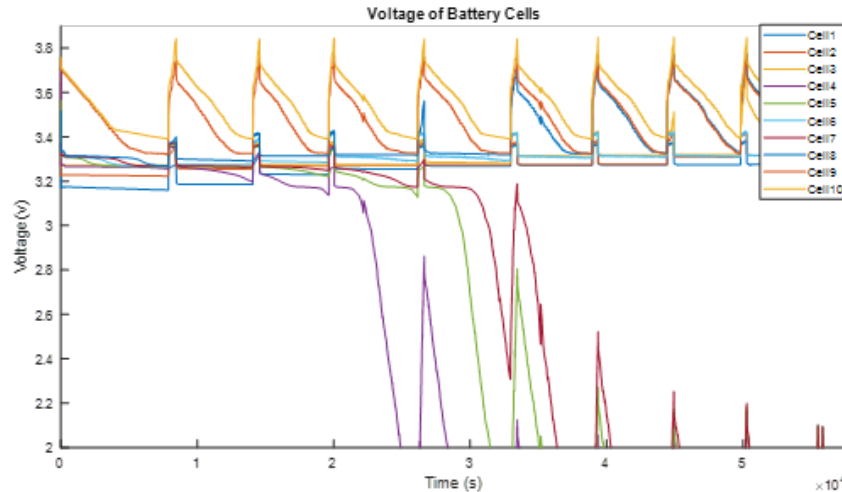


Figure 16. Plot showing Chroma cell emulation on K2 Energy BMS. Abnormal operation of the K2 Energy BMS is observed. Three cells appear to be balancing down despite not being past the balance threshold while the other cells are running and balancing as expected. These cells were brought down to 0 VDC and the simulation was stopped.

3.3.5. Chroma Emulator on NXP BMS

Further demonstration is achieved by testing a BMS manufactured by NXP Semiconductors, model number RDDDRONE-BMS772, that is primarily used in drone applications. There is another project occurring in the lab that employs this BMS so prior to installing it, the emulator was used to study its operation and verify that it behaves as programmed. The data is shown for nothing more than to further demonstrate the application of the battery emulator for a wide range of use cases. The NXP BMS balances 6 cells and controls the recharge or discharge process using onboard solid state switching. Figure 17 shows the cell outputs commanded by the simulation while monitored and balanced by the NXP BMS. The BMS's ability to independently isolate the battery is of interest since this type of operation could compete with control from a higher-level control system. The interaction of two competing controllers is a use case that always needs to be explored.

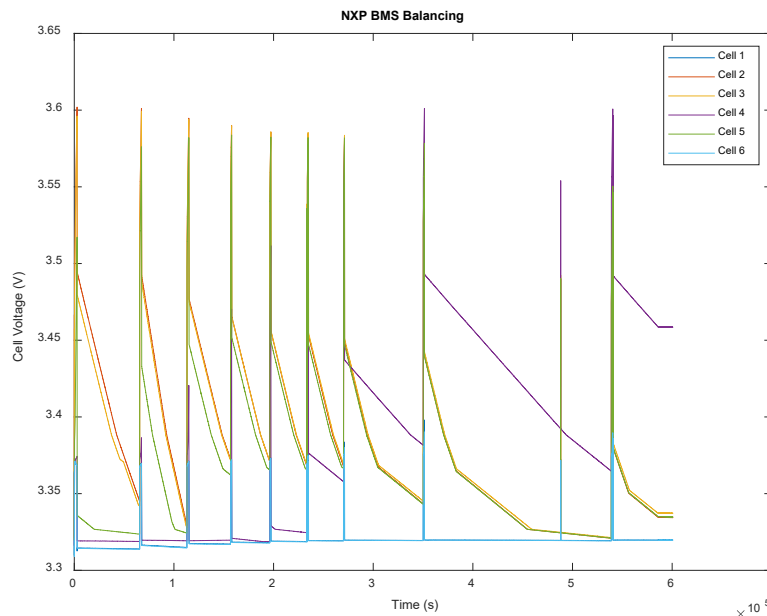


Figure 17. Balance test on a six cell NXP BMS designed for drone applications. Although by the end of this test, the BMS was not fully brought into balance, cells 4 and 5 are brought into balance with cells 2 and 3. In this experiment the recharge cycles were performed using a physical power supply with the emulator acting as a sink. The current supplied is measured and used to update each individual cells SoC.

3.4. Integration with a Power System Controller

In 2019, UTA designed and installed a medium voltage AC/DC testbed that is being used to study the integration and control of distributed power sources and loads. The testbed, which will not be discussed in any detail here, is known as the Intelligent Distributed Energy Analysis Laboratory (IDEAL) and it has been well documented in (Johnston 2022, Johnston 2020, Johnston 2020, Johnston 2020). Within the testbed, there is a 1 kVDC lithium-iron-

phosphate (LFP) battery that is used both as a dedicated source and as a buffer to the primary AC source. The K2 Energy BMS has been previously installed on the battery and it has been integrated into the IDEAL control system so that every individual cell's voltage can be monitored in RT. The BMS can interface with external contactors to isolate the battery autonomously in the event something falls out of the acceptable bounds but none of those features are employed within IDEAL. The IDEAL controller monitors every cell and makes RT decisions on how to utilize the battery based off the mode of operation, load priority, and battery SoC, among other factors. A snapshot of the LabVIEW Virtual Instrument (VI) panel that monitors the BMS is shown in Figure 18. The IDEAL control system was designed and developed with the battery installed on the testbed and while everyone is always careful during commissioning of any software changes, it is difficult to study extreme conditions as it could become an unsafe situation if the controller does not respond as it is supposed to. The emulator being implemented here is a perfect solution for developing these types of system level controllers. The scenarios demonstrated in the previous sections can be emulated and the control system's response will be able to be debugged in a safe and effective manner. Future work will discuss the implementation of the emulator in the development of control algorithms employed in IDEAL.

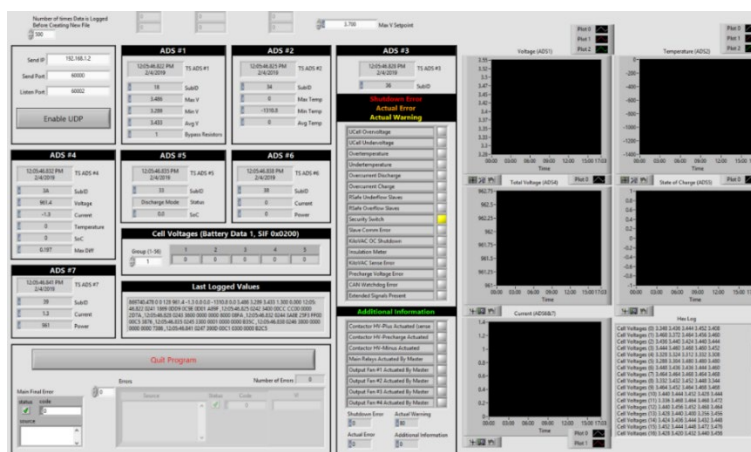


Figure 18. LabVIEW VI used to measure data from the K2 Energy BMS's fiber optic data stream. This VI is used to plot cell data in RT and transmit cell maximum and minimum voltage values to the IDEAL power system controller.

4. Conclusion

This report has presented the rationale, design, and some preliminary results obtained from a battery emulator that is being used to study how BMSs perform in short- and long-term modes of operation. The testbed can be used to study any BMS for use in any application quickly and safely. A brief demonstration of how the emulated battery will be integrated into the design and development of power system controller algorithms. There are many BMSs offered commercially and more that are being developed each day. The lack of standards against which all BMSs are designed makes each one unique. Because batteries do have inherent safety concerns, it is critical that the BMS used is fully vetted against all possible scenarios. Further, any shipboard power system controller that is operating a battery must be vetted in a safe and reliable manner. As battery voltages increase, as high as 1 kVDC, and as the stored energy increases, the need for management and safety grows exponentially. The work presented here has shown a few possible options for designing a battery emulator that can be used to safely and reliably study BMSs. Only preliminary results have been presented and future work is planned to integrate these systems with different on-board ship controllers to test not only the BMS but also how a controller may respond and act to improve the operation of these systems.

Acknowledgements

This material is based upon work supported by General Technical Services (GTS) under subcontract number GTS-S-20-156. The prime sponsor is the Naval Surface Warfare Center – Philadelphia Division.

References

D.A. Wetz, M.J. Martin, C.L. Williams, D.A. Dodson, and J.M. Heinzl, 'Design of Two 1000 V Batteries for Evaluation as Pulsed Power Prime Power Supplies,' 7th Hypervelocity Gun Weapon System Workshop, September 20 – 21, 2016, Laurel, Maryland.

D.A. Dodson, D.A. Wetz, J.L. Sanchez, C.G. Gnegy-Davidson, M.J. Martin, B. Adams, A.N. Johnston, J.M. Heinzl, S. Cummings, N. Frank, N.A. Rahim, and M. Davis, 'Design and Evaluation of a 1000 V Lithium-Ion Battery,' Naval Engineers Journal, Vol. 131, No. 3, September 2019, pp. 107 – 119.

T. Moloughney, '2021 Lucid Air Dream Edition Revealed: Range, Pricing, Specs, And More,' InsideEVs, <https://insideevs.com/news/443057/lucid-air/>, September 9, 2020.

L. Buccolini, S. Orcioni, S. Longhi and M. Conti, "Cell Battery Emulator for Hardware-in-the-Loop BMS Test," 2018 IEEE International Conference on Environment and Electrical Engineering and 2018 IEEE Industrial and Commercial Power Systems Europe (EEEIC / I&CPS Europe), Palermo, 2018, pp. 1-5, doi: 10.1109/EEEIC.2018.8493731.

A. Colthorpe, 'Arizona battery fire's lessons can be learned by industry to prevent further incidents, DNV GL says,' <https://www.energy-storage.news/arizona-battery-fires-lessons-can-be-learned-by-industry-to-prevent-further-incidents-dnv-gl-says/>, [online], August 30, 2022.

J. Cao, N. Schofield and A. Emadi, "Battery balancing methods: A comprehensive review," 2008 IEEE Vehicle Power and Propulsion Conference, Harbin, 2008, pp. 1-6, doi: 10.1109/VPPC.2008.4677669.

S. Cummings, 'South Korea Identifies Top 4 Causes for ESS Fires,' <https://liiontamer.com/south-korea-identifies-top-4-causes-that-led-to-ess-fires/>, [online], August 30, 2022.

IRCLASS, 'Guidelines on Battery Powered Vessels,' Indian Register of Shipping, IRS-G-SAF-04, 2019, https://www.irclass.org/media/4153/guidelines-for-battery-powered-vessels_2019.pdf, [online], August 30, 2022.

'Battery pack BMS failure mode,' <https://www.batterypackequipment.com/news/Battery-pack-BMS-failure-mode.html?btwaf=88651701>, [online], August 30, 2022

J. Chung, 'Battery Incident Root Cause Analysis and Review the Certifications,' https://www.nasa.gov/sites/default/files/atoms/files/batt_inc_root_cause_analysis_rev_certs_jchung.pdf, [online], August 30, 2022.

C. D. Tschritter, D. A. Wetz, G. K. Turner and J. M. Heinzl, "Battery Management System (BMS) Test Stand Utilizing a Hardware-in-the-Loop (HIL) Emulated Battery," 2021 IEEE Electric Ship Technologies Symposium (ESTS), 2021, pp. 1-8, doi: 10.1109/ESTS49166.2021.9512327.

Chroma, "16CH Battery Cell Simulator" 87001 User's manual, April 2019

Hioki, "Battery Cell Voltage Generator," SS7081C961-00 20-04H Instruction Manual, April 2020

"IO991: Battery Emulation I/O Module," Speedgoat. [Online]. Available: <https://www.speedgoat.com/products/battery-management-systems-io991>. [Accessed: 28-Feb-2021].

A.N. Johnston, Z.R. Bailey, D.A. Wetz, G.K. Turner, and J.M. Heinzl, 'Design and Commissioning of a Medium Voltage Testbed with Emulated Pulsed Loads,' Accepted for publication in the Naval Engineers Journal, March 2022, publication pending.

A.N. Johnston, D.A. Wetz, R. Madani, A. Davoudi, G.K. Turner, D.A. Dodson, B.J. McRee, Z. Bailey, D. Pullaguram, J.M. Heinzl, M. Giuliano, and C.M. Schegan, 'Mitigating Transient Loads in Medium-Voltage Direct Current Microgrids,' Proceedings of the 2020 American Society of Naval Engineers (ASNE) Advanced Machinery Technology Symposium (AMTS), October 7-8, 2020, Philadelphia, Pennsylvania.

A.N. Johnston, D.A. Wetz, Z. Bailey, D.A. Dodson, B.J. McRee, and J.M. Heinzl, 'A Medium Voltage, Distributed Power Generation Testbed Deploying Transient Loads,' Proceedings of the International Ship Control Systems Symposium (iSCSS), October 6 – 8, 2020, Delft, Netherlands.